

# MAUVE: Human-Machine Divergence Curves for Evaluating Open-Ended Text Generation

Krishna Pillutla<sup>♡</sup> Swabha Swayamdipta<sup>♣</sup> Rowan Zellers<sup>♡</sup> John Thickstun<sup>♡</sup>  
Yejin Choi<sup>♡♣</sup> Zaid Harchaoui<sup>◇</sup>

<sup>♡</sup>Paul G. Allen School of Computer Science & Engineering, University of Washington

<sup>♣</sup>Allen Institute for Artificial Intelligence

<sup>◇</sup>Department of Statistics, University of Washington

{pillutla, rowanz, thickstn, yejin, zaid}@cs.washington.edu  
swabhas@allenai.org

## Abstract

Despite major advances in open-ended text generation, there has been limited progress in designing evaluation metrics for this task. We propose MAUVE—a metric for open-ended text generation, which directly compares the distribution of machine-generated text to that of human language. MAUVE measures the mean area under the divergence curve for the two distributions, exploring the trade-off between two types of errors: those arising from parts of the human distribution that the model distribution approximates well, and those it does not. We present experiments across two open-ended generation tasks in the web text domain and the story domain, and a variety of decoding algorithms and model sizes. Our results show that evaluation under MAUVE indeed reflects the more natural behavior with respect to model size, compared to prior metrics. MAUVE’s ordering of the decoding algorithms also agrees with that of generation perplexity, the most widely used metric in open-ended text generation; however, MAUVE presents a more principled evaluation metric for the task as it considers both model and human text.<sup>1</sup>

## 1 Introduction

The explosive scales of pre-trained neural language models such as OpenAI’s GPT-3 (Brown et al., 2020) have revealed that left-to-right neural language models can generate text with remarkable quality and coherence. As a result, open-ended text generation has become a newly emerging research focus for applications around story and dialogue generation, where multiple generations are equally plausible, and diversity in generated text is often desired. Despite these advances, however, automatic evaluation metrics for these tasks still consider either a few human references, or none at all (§2);

<sup>1</sup>This is a work-in-progress draft.

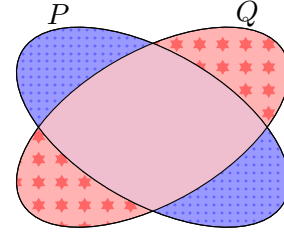


Figure 1: Two different sources which contribute to  $\text{MAUVE}(P, Q)$  for the human text distribution  $P$ , and model text distribution  $Q$ . **Type I Error**: mass of  $P$  not captured by  $Q$ , **Type II Error**: unlikely regions under  $P$  with high probability under  $Q$ , and, **the center** represents how different  $Q$  is from  $P$  on the common regions supported by both. A scalar  $\lambda \in (0, 1)$  quantifies how to attribute the **error in the center** to either Type I or II; different  $\lambda$  values are needed to fully assess the generative model  $Q$  w.r.t. true distribution  $P$ , resulting in a divergence curve. The proposed metric MAUVE is given by the area under this curve, as a scalar summary of the divergence.

neither approach is sufficient to measure the quality and diversity of machine text, as it compares to human text.

We introduce MAUVE, an evaluation metric for open-ended generation specifically designed for addressing these issues. MAUVE directly captures the divergence between the distribution of generated text to the human-written, reference language distribution (§3). Inspired by recent work on evaluating generative models (Sajjadi et al., 2018; Kynkäänniemi et al., 2019; Djolonga et al., 2020) and unlike prior metrics, our metric takes into account two different kinds of errors stemming from systematic differences between the distribution of machine-generated text and that of human language, as illustrated in Fig. 1. Based on the trade-off in the importance assigned to each type of error, we can build a divergence curve between

the two distributions, based on different thresholds for trade-off between the two errors. MAUVE summarizes the divergence between human and machine text as the mean area under this divergence curve. Given neural language models are associated with large distributions which cannot be completely specified, our contributions include a method to operationalize this metric via discretization approaches (Courbariaux et al., 2016).

We provide experiments which compare several decoding approaches on different model sizes on two domains—web text and stories in English (§4). Our results show that evaluation under MAUVE indeed rewards generations from larger models over smaller architectures, confirming trends which have now been established (Brown et al., 2020); these results are more consistent, compared to prior metrics. MAUVE also confirms that decoding approaches which do not rely on the unreliable tail of the model distribution (Holtzman et al., 2020) produce better generations than those which do. While these results are in agreement with those under generation perplexity, the most widely used metric in open-ended text generation, MAUVE presents a more principled evaluation metric for the task as it considers both model and human text, unlike perplexity which only considers model generations. Given our work is still under progress, we conclude with a brief outline of future directions and ethical considerations (§6). Our code is publicly available<sup>2</sup>.

## 2 Background on Open-Ended Text Generation

Language models are probabilistic models which learn a distribution  $Q$  over a text sequence, containing tokens from a fixed vocabulary. The task of open-ended text generation involves decoding under the language model,  $Q$ , i.e. generating text in continuation to a given context<sup>3</sup>. This is typically done by generating one token at each time-step, in a left-to-right fashion, from the learned distribution  $Q$ . The goal, therefore, is to learn a distribution  $Q$  which closely resembles the distribution of human text,  $P$ ; evaluation methods (§2.1) either consider the distributions directly, or samples from it.

<sup>2</sup><https://github.com/krishnap25/mauve-experiments>

<sup>3</sup>Unlike targeted generation tasks like translation or summarization, coherence, creativity, and fluency are the main criteria for open-ended text generation.

**Decoding Approaches** The quality of machine generated text is deeply dependent on the decoding method, for any given trained language model. Decoding involves either maximization under the original distribution  $Q$  (such as greedy decoding) or sampling from it. Other approaches involve modifying  $Q$  either via temperature scaling (Ackley et al., 1985) or simply truncating the unreliable tail probabilities via top- $k$  sampling (Fan et al., 2018), or nucleus sampling (Holtzman et al., 2020). Finally, Martins et al. (2020) propose a method to natively train and sample from a sparse text distribution, called entmax sampling. Decoding strategies are summarized in Table 7 and discussed in detail in Appendix §A.2.

### 2.1 Evaluating Open-Ended Generation

We classify existing evaluation metrics of text generation into three categories: evaluation of generated text with respect to (a set of) reference text sample(s) (§2.1.1), or with respect to the entire model distribution ( $Q$ ; §2.1.2), or the evaluation of human text with respect to a re-calibrated model distribution (§2.1.3). Table 1 summarizes existing automatic metrics as well as our proposed metric, MAUVE (§3).

#### 2.1.1 Machine Text vs. Reference Text

Classical metrics such as BLEU (Papineni et al., 2002), ROUGE (Lin, 2004), METEOR (Banerjee and Lavie, 2005) assume the existence of one true reference, or a small set of human references. Designed for directed generation tasks like translation and summarization, these metrics reward task-specific properties of the generated text, such as, meaning-preserving translations of the source text, or succinct and faithful summaries of the source. This paradigm is unsuitable in open-ended generation where multiple continuations are possible for a given context, and creative generations are desirable.

#### 2.1.2 Model Distribution on Model Text

It is more natural to evaluate based on the entire learned distribution  $Q$ , instead of a few reference samples. The most widely used metric in this category is the generation perplexity (Gen. PPL): it is based on the likelihood of generated text under the original  $Q$  from the language model. For instance, Holtzman et al. (2020) compute the likelihood (or perplexity) of generated text under  $Q$ , and compare it to the likelihood of human text under the

Metric	References	Measures	Model Text	Human Text
Generation Perplexity	(Fan et al., 2018; Holtzman et al., 2020)	Plausibility of generation	✓	
Zipf Coefficient	(Holtzman et al., 2020)	Word usage statistics	✓	
Self-BLEU	(Zhu et al., 2018)	Diversity of generation	✓	
Distinct $n$ -gram fraction	(Holtzman et al., 2020; Welleck et al., 2020b; Martins et al., 2020)	Repetitiveness of generation	✓	
Non-termination Ratio	(Welleck et al., 2020a)	Consistency	✓	
Support per generation	(Massarelli et al., 2019)	Verifiability recall	✓	
Support per verified	(Massarelli et al., 2019)	Verifiability precision	✓	
$\varepsilon$ -perplexity	(Martins et al., 2020)	Language modeling quality		✓
Sparsemax Score	(Martins et al., 2020)	Language modeling quality		✓
Jensen-Shannon Divergence	(Martins et al., 2020)	Language modeling quality		✓
MAUVE	Our Work	Generation quality and diversity	✓	✓

Table 1: Summary of automated metrics for evaluating open-ended text generation. Classical metrics (such as BLEU; Papineni et al., 2002) which are task-specific and unsuitable for open-ended generation, as well as metrics specific to particular domains such as story generation have been omitted.

same  $Q$ . However, rewarding the likelihood (i.e. perplexity) of machine generated text results in low-diversity generated sequences that have been found empirically to be degenerate or repetitive, and therefore atypical in natural language (Holtzman et al., 2020). Moreover, perplexity also penalizes rare words, common in creative language.

Other metrics in this category simply compute the statistics of generated text, such as repetition frequency (REP), ratio of unique  $n$ -grams (Distinct- $n$ ), or how likely the text is to terminate (Welleck et al., 2020b), or the verifiability of text under a given knowledge base (Massarelli et al., 2019). Holtzman et al. (2020) use the Zipf coefficient to measure how likely, under the model distribution, words are frequent in the training corpus. While such metrics can reveal important properties of machine text, these are not stand-alone estimators of its quality. Another metric under this category is Self-BLEU (Zhu et al., 2018) which measures the diversity of generated text, by computing the average BLEU score between every pair of machine generations under the same context; the set of machine generations thereby approximates the model distribution. However, it is still subject to the limitations of BLEU (Mathur et al., 2020). Overall, such metrics only provide a narrow aspect of machine text properties, such as the amount of repetitions, without providing more systematic measures of how the distribution of machine language deviates from the distribution of human language.

### 2.1.3 Recalibrated Model Distribution on Reference Text

The final category of metrics compute the likelihood of reference or human text (typically) under a recalibrated model distribution. These include three metrics used in Martins et al. (2020):  $\varepsilon$ -perplexity ( $\varepsilon$ -PPL), sparsemax score (SP), and the Jensen-Shannon divergence (JS).  $\varepsilon$ -perplexity computes the perplexity of human text after adding a Laplace smoothing to  $Q$ . Sparsemax score is a bounded metric designed for sparse text generated by entmax sampling; it indicates the quality of human text after the application of the entmax transformation (Peters et al., 2019) to  $Q$ . JS measures the reduction of uncertainty about the model distribution when we see samples of human reference text. Given these metrics are designed for sparse text generation, by definition, they cannot apply to deterministic decoding methods such as beam search, since where a next token distribution might not always be available. Moreover these metrics tend to reward text generated via pure sampling and greedy decoding, which has been shown to be “degenerate” (Holtzman et al., 2020).

## 3 MAUVE: Mean Area Under DiVergence CurvEs

In contrast to prevalent metrics of open-ended text generation, we propose a metric, MAUVE which is based on the model distribution  $Q$  over *both* machine-generated as well as reference human text; the latter is used to approximate the true distribution,  $P$ . The evaluation of generative models must

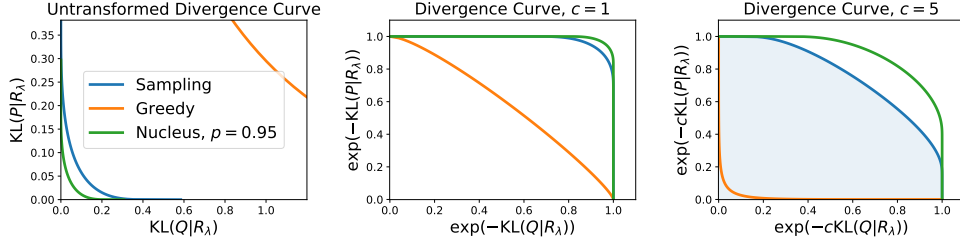


Figure 2: **Left:** The curve showing  $(\text{KL}(Q|R_\lambda), \text{KL}(P|R_\lambda))$ , the formalization of Type I and Type II errors, respectively on web text generated by GPT-2 large. Smaller is better. **Middle:** The corresponding divergence curves for  $c = 1$ . Since  $x \mapsto e^{-x}$  is monotonic decreasing, larger is better is this curve. The divergence curve is now fully contained in the unit rectangle  $[0, 1]^2$ . **Right:** The same divergence curves for  $c = 5$ . Changing  $c$  maintains the same order but allows for a more meaningful comparison of the numerical value of MAUVE. MAUVE is calculated as the area under the divergence curve; the shaded region denotes the MAUVE score of sampling.

include an assessment of what parts of the true distribution the model is able to approximate well, and what other parts of the distribution it is not.

### 3.1 Informal Description

Consider the task of assessing how good a text generative model distribution  $Q$  is to the true distribution  $P$  of text written by humans. As highlighted in Figure 1, there are two obvious sources of errors:

- (I)  $Q$  places high mass on text which is unlikely under  $P$ , or,
- (II)  $Q$  does not capture a part of  $P$ .

The former, which leads to false positives or type I errors, can occur because sampling algorithms tend to generate text with semantic repetitions (Dinan et al., 2019; Holtzman et al., 2020; Welleck et al., 2020b), which are highly unlikely to be written by humans<sup>4</sup>. The latter case results in false negatives, also known as type II errors. These can occur, for instance, because some pieces of plausible human text cannot be generated by sparse decoding algorithms such as nucleus (Holtzman et al., 2020) or entmax (Martins et al., 2020) sampling. Indeed, this is why the perplexity cannot be used to evaluate sparse language models (Martins et al., 2020).

When  $P$  and  $Q$  place different non-zero amounts of probability mass on some text, we cannot attribute this discrepancy between  $P$  and  $Q$  uniquely as a false positive or a false negative. Following recent work (Sajjadi et al., 2018; Djolonga et al., 2020), we must consider a family of type I and

II error values for different  $\lambda \in (0, 1)$ , where we designate  $\lambda$ -fraction of this error as type I and a  $(1 - \lambda)$ -fraction as type II.

### 3.2 Formal Definition of MAUVE

To formalize the above discussion, we consider a mixture  $R_\lambda = \lambda P + (1 - \lambda)Q$  for some  $\lambda \in (0, 1)$ . We measure the type I and II errors by how far  $Q, P$  are from  $R_\lambda$  in terms of the Kullback-Leibler (KL) divergence, denoted  $\text{KL}(\cdot|\cdot)$ .

Concretely,  $\text{KL}(Q|R_\lambda)$  penalizes  $Q$  if there exists text  $\mathbf{x}$  such that  $Q(\mathbf{x})$  is large but  $R_\lambda(\mathbf{x})$  is small. This measures the type I error. Similarly,  $\text{KL}(P|R_\lambda)$  measures the type II error.

The errors  $\text{KL}(Q|R_\lambda), \text{KL}(P|R_\lambda)$  are not unique since  $\lambda$  was arbitrary. By varying  $\lambda \in (0, 1)$  we get a divergence curve,

$$\mathcal{C}(P, Q) = \left\{ (e^{-c\text{KL}(Q|R_\lambda)}, e^{-c\text{KL}(P|R_\lambda)}) : R_\lambda = \lambda P + (1 - \lambda)Q, \lambda \in (0, 1) \right\},$$

where  $c > 0$  is a hyperparameter for scaling. The transformation  $x \mapsto e^{-cx}$  is monotonic for all  $c > 0$ , i.e., it preserves order. Furthermore, the transformed curve  $\mathcal{C}(P, Q)$  lies entirely in the unit square  $[0, 1]^2$ .

Finally, we define the metric  $\text{MAUVE}(P, Q) \in [0, 1]$ , as the area under the divergence curve  $\mathcal{C}(P, Q)$ , as a scalar summary of the divergence curve. A larger value of MAUVE denotes better performance. See Figure 2 for an example.

We note that this divergence curve contains more information than KL divergence  $\text{KL}(P|Q)$ , which can be obtained from the second coordinate of the curve  $\mathcal{C}(P, Q)$  as  $\lambda \rightarrow 0$ , and the reverse KL divergence  $\text{KL}(Q|P)$  which can be obtained from the first coordinate of the curve  $\mathcal{C}(P, Q)$  as  $\lambda \rightarrow$

<sup>4</sup>Let text  $\mathbf{x}$  with  $P(\mathbf{x}) \gg 0$  be the positive class and  $P(\mathbf{x}) \approx 0$  be the negative class. If  $Q(\mathbf{x}) \gg 0$  for some negative  $\mathbf{x}$ , then the model incorrectly considers it a positive, i.e., a false positive, and  $\mathbf{x}$  can never be generated by  $P$ .

1. Further, the Jensen-Shannon (JS) divergence  $JS(P, Q) = (\text{KL}(P|R_{1/2}) + \text{KL}(Q|R_{1/2}))/2$ , can be obtained from the two coordinates of  $\mathcal{C}(P, Q)$  at  $\lambda = 1/2$ . MAUVE summarizes *all* of the divergence curve  $\mathcal{C}(P, Q)$ , not just particular points on the curve, as done by the KL or JS divergences.

**Remark 1.** *The divergence curve  $\mathcal{C}(P, Q)$  encodes the Pareto frontier of  $(\text{KL}(P|R), \text{KL}(Q|R))$  for all distributions  $R$ , not just mixtures of the form  $R_\lambda$ . We prove this in §B.*

### 3.3 MAUVE for Evaluating Open-Ended Text Generation

Next, we turn to efficiently computing MAUVE towards the evaluation of open-ended text generation.

In this case, a language model together with a decoding algorithm induces a distribution over possible generations. However, for a moderately large length of a sentence, the size of the support of this distribution is intractably large, particularly for neural language models. Hence, the divergence curve for MAUVE cannot be tractably computed in closed form.

We overcome this problem by using a finite dimensional, dense representation of text: the embedding of the hidden state for the sentence under a neural language model, similar to the method from Zhang et al. (2020). However, estimating the KL divergence between two high dimensional distributions from samples is still extremely challenging.

We perform one further approximation for computation tractability—we quantize the distribution of hidden states into a discrete multinomial distribution. Towards this, we consider three different quantization methods:

1. *k*-means: We cluster the hidden representations using *k*-means, and represent them by their cluster membership to get a discrete distribution with as many dimension as the number of clusters. We call this MAUVE-*k*-means.
2. Deep Residual Mixture Models (DRMM): As a generalization of *k*-means, we train a deep generative model known as DRMM (Hämäläinen and Solin, 2020). We convert the soft clustering so obtained into a hard clustering by assigning each point to its most likely cluster, and quantize the data using the cluster membership. We call this MAUVE-DRMM.

3. Lattice quantization of learnt features: We learn a feature representation of the hidden states using a deep network which maintains the neighborhood structure of the data while encouraging the features to be uniform (Sablayrolles et al., 2019). We simply quantize the data on a lattice. We call this MAUVE-Lattice.

## 4 Experiments

We present experiments to show the ability of MAUVE to evaluate the quality of generated text for various state-of-the-art decoding algorithms and models. We compare MAUVE to existing methods of text generation (see §2.1) across decoding methods and model architectures.

### 4.1 Data and Experimental Setup

We consider open-ended text generation under two domains: web text and the story domain. We use size-variants of the GPT-2 model (Radford et al., 2019) in each setting. At decoding time, we explore a text continuation setting, conditioned on a prompt containing human-written text. All experiments were built using pretrained models and functions available under the HuggingFace Transformers library (Wolf et al., 2020).

**Web Text Generation** We consider the publicly available analogue of the Webtext dataset.<sup>5</sup> Given its similarity to the training data of GPT-2, we do not finetune GPT-2 on this data, and simply use the released GPT-2 architecture in its small and large variants. At generation time, we use as prompts the first 10 tokens of each of the 5000 the test examples of the Webtext corpus. The machine generations are allowed to be up to 1024 tokens long. As human-written continuations for comparison, we use the corresponding test examples up to a maximum of 1024 tokens.

**Story Continuation** Given a situation and the starting of a story as a prompt, the goal is the continue the story. Here, we use the GPT-2 medium architecture, finetuned on the training set of the WritingPrompts dataset (Fan et al., 2018). We use as a generation prompt the first 50 tokens of 5000 randomly chosen samples from the test set of WritingPrompts. The machine generations are allowed to be up to 512 tokens long. The corresponding

<sup>5</sup><https://github.com/openai/gpt-2-output-dataset>

		Gen. PPL	Zipf Coef.	REP	Distinct-4	Self-BLEU	SP	JS	$\varepsilon$ -PPL	MAUVE
GPT-2 small	Sampling	79.351 <sub>1.286</sub>	0.925 <sub>0.000</sub>	0.001 <sub>0.000</sub>	0.945 <sub>0.001</sub>	0.313 <sub>0.002</sub>	0.653	0.425	19.401	0.498 <sub>0.010</sub>
	Greedy	1.136	1.061	0.942	0.047	0.579	0.431	0.394	1049.589	0.008
	Nucleus, $p = 0.95$	29.224 <sub>0.228</sub>	<b>0.957</b> <sub>0.001</sub>	0.005 <sub>0.001</sub>	0.900 <sub>0.002</sub>	<b>0.389</b> <sub>0.003</sub>	0.653	0.419	21.928	0.807 <sub>0.008</sub>
	Human	19.302	0.963	0.002	0.878	0.382				
GPT-2 large	Sampling	34.433 <sub>0.364</sub>	0.946 <sub>0.001</sub>	<b>0.002</b> <sub>0.000</sub>	0.918 <sub>0.001</sub>	0.347 <sub>0.001</sub>	<b>0.679</b>	0.381	<b>12.658</b>	0.782 <sub>0.012</sub>
	Greedy	1.147	1.041	0.888	0.074	0.486	0.483	<b>0.359</b>	580.020	0.011
	Nucleus, $p = 0.95$	<b>13.638</b> <sub>0.121</sub>	0.970 <sub>0.000</sub>	0.007 <sub>0.001</sub>	<b>0.865</b> <sub>0.003</sub>	0.410 <sub>0.003</sub>	0.679	0.374	14.938	<b>0.909</b> <sub>0.006</sub>
	Human	12.602	0.963	0.002	0.878	0.382				

Table 2: Comparing evaluation metrics across different decoding approaches, as well as different GPT-2 architectures for web text generations. Subscripts indicate the s.d. across 5 runs for the sampling-based methods; greedy decoding, being deterministic, always returns the same value for a given model. For nucleus sampling, we show the best hyperparameter value from  $\{0.8, 0.9, 0.92, 0.95, 0.99\}$  as per MAUVE. Boldfaced numbers indicate performance closest to the human reference when applicable. MAUVE shows that larger models perform better, across decoding approaches; moreover, nucleus sampling is the best decoding metric.

	Gen. PPL	Zipf Coef.	REP	Distinct-4	Self-BLEU	SP	JS	$\varepsilon$ -PPL	MAUVE
Sampling	27.188 <sub>0.093</sub>	1.031 <sub>0.001</sub>	<b>0.001</b> <sub>0.000</sub>	0.833 <sub>0.001</sub>	0.518 <sub>0.003</sub>	<b>0.642</b>	0.430	<b>18.987</b>	0.905 <sub>0.010</sub>
Greedy	1.557	1.253	0.988	0.101	0.742	0.415	<b>0.406</b>	1267.401	0.005
Nucleus, $p = 0.95$	<b>15.408</b> <sub>0.099</sub>	<b>1.067</b> <sub>0.001</sub>	0.003 <sub>0.000</sub>	<b>0.775</b> <sub>0.002</sub>	<b>0.589</b> <sub>0.005</sub>	0.642	0.424	22.509	<b>0.920</b> <sub>0.004</sub>
Human	18.124	1.052	0.001	0.783	0.571				

Table 3: Comparing evaluation metrics across different decoding approaches, on the GPT-2 medium architecture for story continuation on the WritingPrompts dataset (Fan et al., 2018). Subscripts indicate the s.d. across 5 runs for the sampling-based methods; greedy decoding, being deterministic, always returns the same value for a given model. For nucleus sampling, we show the best hyperparameter value from  $\{0.9, 0.2, 0.95\}$  as per MAUVE. Boldfaced numbers indicate performance closest to the human reference when applicable. MAUVE favors nucleus sampling over pure sampling and greedy decoding.

test examples are used of WritingPrompts are used as human-written continuations up to a maximum of 512 tokens.

**Decoding Algorithms** We generate text by forward sampling from the language model (denoted “sampling”) or a reshaped language model obtained by a truncation heuristic nucleus sampling (Holtzman et al., 2020). We also consider greedy decoding as a likelihood maximization-based alternative to text generation. The finetuning hyperparameters are detailed in §C.

**Hyperparameters of MAUVE** We compute MAUVE with 5000 machine generations and human samples each arising from the common prompts. MAUVE- $k$ -means is computed using  $k$ -means implemented in FAISS (Johnson et al., 2019). Prior to clustering, we reduce the dimensionality of the hidden state representation with PCA to contain 90% of the variance and normalize the features to unit  $\ell_2$  norm. We use MAUVE-DRMM with 3 layers and 10 components per layer for a total of  $10^3$  clusters. The DRMM model is trained for 20 epochs. For quantization, we assign each point to its most likely cluster. For MAUVE-Lattice, we train a 4-dimensional feature representation of the

hidden states for for 200 epochs. We then quantize them using a lattice spherical quantizer into 744 bins. Further details of each method and of the hyperparameters can be found in §C.

We find in §4.4 that all discretization algorithms perform similarly. Hence, unless specified otherwise, we use MAUVE- $k$ -means with  $k = 500$  as our default for its ease of computation. We fix  $c = 5$  throughout as we observed that this

**Reproducibility** We generate five different continuations for each prompt using different random seeds. We present here the mean, and where applicable, the standard deviation of each metric over the five sets of generations.

## 4.2 Baseline Evaluation Metrics

In this work, we compare MAUVE with the following automatic metrics to evaluate the quality of generations (cf. §2.1; Table 1):

- Model text: generation perplexity (Gen. PPL), Zipf coefficient, Self-BLEU, REP (repetition frequency), and Distinct-4 ,
- Human text:  $\varepsilon$ -perplexity ( $\varepsilon$ -PPL), Sparsemax score (SP), and Jensen-Shannon divergence (JS).

	Gen. PPL	Zipf Coef.	REP	Distinct-4	Self-BLEU	SP	JS	$\varepsilon$ -PPL
Web text	0.83	0.65	0.47	0.74	0.57	0.58	-0.47	0.42
Stories	0.69	0.94	0.59	0.75	0.9	0.78	-0.75	0.78

Table 4: Spearman rank correlation between MAUVE and existing metrics. All correlations have  $p$ -value  $< 0.05$  except  $\varepsilon$ -PPL on web text. The table shows GPT-2 large for web text generation and GPT-2 medium for story generation.

For the second category, we compute the metrics on the test set for each task using directly the reshaped or truncated model probabilities from which generations are sampled. We compute Gen. PPL as the perplexity of the model text under the original model it is sampled from (without reshaping or truncation), i.e. the original GPT-2 model.

**Interpreting Results** Better performance is indicated by larger values of MAUVE and SP but smaller values of  $\varepsilon$ -PPL and JS. Other metrics  $\mu$  such as Gen. PPL compute metrics on the model text; the values of these metrics for a decoding algorithm are only meaningful in comparison to the value of this metric on human text. Therefore, we prefer smaller values of  $|\mu_{\text{model}} - \mu_{\text{human}}|$ .

### 4.3 Comparison of Metrics

Tables 2 and 3 present our comparisons of MAUVE to the prior evaluation metrics (§4.2) on web text generation and story continuation, respectively.

First and foremost, we observe that among the decoding approaches, nucleus sampling achieves the best MAUVE followed by sampling and lastly by greedy decoding. This trend is consistent with the perplexity of the generated text under the original model they were generated from as well as the fraction of distinct 4-grams. On the other hand, JS favors greedy decoding, which is known to produce extremely degenerate text (Welleck et al., 2020b). Likewise,  $\varepsilon$ -PPL favors pure sampling, which also produces somewhat degenerate text (Holtzman et al., 2020), while SP appears to be unable to distinguish between pure sampling and nucleus sampling. This makes SP, JS and  $\varepsilon$ -PPL unsuitable as metrics to evaluate the quality of generated text.

While most metrics show expected behavior across model architectures (larger models produce better generations), Zipf coefficient and Self-BLEU prefer generations from GPT-2 small over GPT-2 large. This indicates that while metrics based on word/token statistics are important diagnostic tools, they do not capture the quality of generated text

entirely.

We compare the Spearman rank correlation between MAUVE and existing metrics in Table 4. We see a strong, statistically significant correlation (0.83) with the generation perplexity in the case of web text while the correlation in the case of story generation is slightly weaker at 0.69. We note that Distinct-4 and Self-BLEU show strong correlations with MAUVE. However, Table 2 offers a cautionary note where Self-BLEU ranked generations from GPT-2 small over those from GPT-2 large.

**MAUVE is Sensitive to Generation Length** We plot in Fig. 3 (Left) how MAUVE varies with the maximum generation length for pure, nucleus and entmax sampling.

We observe for each sampling algorithm that MAUVE reduces as the length of generations increases. This shows that the distribution of generated text drifts farther away from human text as the distribution length increases.

Second, we observe that entmax sampling scores the highest until length 512 after which its performance sharply drops. This is explained by the distribution of sentence lengths in Fig. 3 (Right). The generations from the entmax sampler are, on aggregate, shorter in length than human text. When the maximum generation length is 512 tokens or smaller, this difference in distribution is erased due to clipping each generation at 512 tokens long, and the entmax generations score highly as per MAUVE. This shows that MAUVE is sensitive to the length distribution of the generated text compared to that of human text. This is in contrast to metrics such as  $\varepsilon$ -PPL and SP which depend only on the model, not on the generated text.

	DRMM	Lattice
Web text	0.97	0.93
Stories	0.78	0.89

Table 5: Spearman rank correlation between MAUVE- $k$ -means and other quantization schemes. All entries have a  $p$ -value of  $< 0.005$ .

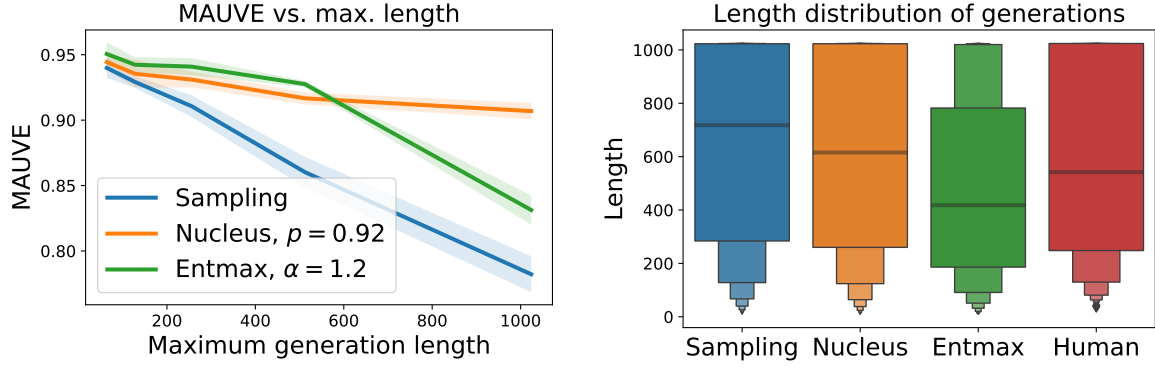


Figure 3: **Left:** MAUVE as the maximum generation length is varied. The shaded region indicates one s.d. over 5 runs. **Right:** length statistics of generated text.

	Correlation
$k = 100$	0.94
$k = 250$	1.0
$k = 1000$	0.94
$k = 1500$	1.0
$k = 2000$	1.0

Table 6: Spearman rank correlation between MAUVE- $k$ -means with  $k = 500$  and other values of  $k$ . All entries have a  $p$ -value of  $< 0.005$ .

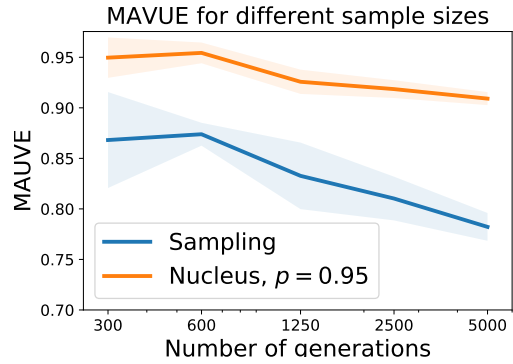


Figure 4: Effect of the sample size on MAUVE.

#### 4.4 Hyperparameter Study

We now study the effects of varying the different hyperparameters involved in the discretization under MAUVE.

**Quantization and Number of Clusters** We see in Table 5 that both MAUVE-DRMM and MAUVE-Lattice correlate very strongly with MAUVE- $k$ -means. Next, we see in Table 6 that MAUVE- $k$ -means with different  $k$  correlates nearly perfectly with  $k = 500$ . We note, however, the Spearman rank correlation measures the agreement in the ranking induced by different variants of MAUVE; the absolute values could be different. Overall, these results indicate that MAUVE is robust to choice of hyperparameters, as long as there is a consistent selection.

**Effect of Number of Generations** We plot in Figure 4 the value of MAUVE versus the sample size  $n$ , with the number of clusters chosen as  $k = n/10$ . We observe that a smaller sample size gives an optimistic estimate of MAUVE; this is consistent with (Djolonga et al., 2020, Prop. 8). We also note that a smaller sample size leads to a larger variance in MAUVE.

## 5 Additional Related Work

Evaluation of generative models is an active area of research in computer vision, where generative adversarial networks (Goodfellow et al., 2014) are commonly used. However, metrics such as Inception Score (IS; Salimans et al., 2016) are designed for supervised classification settings, and thus inappropriate for text generation. The Frechet Distance (FID; Heusel et al., 2017) and its unbiased counterpart, the Kernel Inception Distance (Bińkowski et al., 2018) are both used for evaluating generative models, but unlike MAUVE, do not take into account a trade-off between different kinds of errors between the learned and a reference distribution. Sajjadi et al. (2018) and Kynkäänniemi et al. (2019) both proposed metrics based on precision-recall curves. Djolonga et al. (2020) proposed a framework which encompassed both these works. MAUVE extends the above line of work, and is operationalized as a metric for evaluating open-ended text generation, applicable for data generated by large-scale neural language models.

## 6 Discussion

We presented MAUVE, a metric for evaluating open-ended text generation. In our experiments, we used MAUVE to compare different decoding methods, models, and hyperparameters within each setting. Our metric is associated with certain hyperparameters such as number of generation samples to be considered for obtaining meaningful clusters, and the parameters of the clustering approach itself.

The investigation of the alignment of MAUVE with human assessment of machine-generated text through a human evaluations would be an interesting venue for future work. Factors like length of text, which may determine the quality of human assessment (Ippolito et al., 2020), could be taken into consideration in the human evaluations.

**Ethical Implications** Our metric rewards model text which resembles human-authored text. However, we acknowledge the risks of rewarding systems that try to mimic humans, which is the ultimate goal of open-ended text generation (Bender et al., 2021). While our research is important for developing better language generators, we also encourage the community to pay attention to the development of technology that can reliably distinguish between human and machine text. We leave the extension of our method towards building such systems to future work.

## Acknowledgments

This work was supported by NSF CCF-2019844, the DARPA MCS program through NIWC Pacific (N66001-19-2-4031), the CIFAR program “Learning in Machines and Brains”, a Qualcomm Innovation Fellowship, and faculty research awards.

## References

- David H Ackley, Geoffrey E Hinton, and Terrence J Sejnowski. 1985. [A learning algorithm for boltzmann machines](#). *Cognitive science*, 9(1):147–169.
- Satanjeev Banerjee and Alon Lavie. 2005. [METEOR: An automatic metric for MT evaluation with improved correlation with human judgments](#). In *Proceedings of the ACL Workshop on Intrinsic and Extrinsic Evaluation Measures for Machine Translation and/or Summarization*, pages 65–72, Ann Arbor, Michigan. Association for Computational Linguistics.
- Emily M Bender, Timnit Gebru, Angelina McMillan-Major, and Shmargaret Shmitchell. 2021. [On the dangers of stochastic parrots: Can language models be too big?](#) In *Proc. of FAccT*.
- Mikołaj Bińkowski, Danica J. Sutherland, Michael Arbel, and Arthur Gretton. 2018. [Demystifying MMD GANs](#). In *Proc. of ICLR*.
- Mark Braverman, Xinyi Chen, Sham M. Kakade, Karthik Narasimhan, Cyril Zhang, and Yi Zhang. 2019. [Calibration, entropy rates, and memory in language models](#).
- Tom B. Brown, Benjamin Mann, Nick Ryder, Melanie Subbiah, Jared Kaplan, Prafulla Dhariwal, Arvind Neelakantan, Pranav Shyam, Girish Sastry, Amanda Askell, Sandhini Agarwal, Ariel Herbert-Voss, Gretchen Krueger, Tom Henighan, Rewon Child, Aditya Ramesh, Daniel M. Ziegler, Jeffrey Wu, Clemens Winter, Christopher Hesse, Mark Chen, Eric Sigler, Mateusz Litwin, Scott Gray, Benjamin Chess, Jack Clark, Christopher Berner, Sam McCandlish, Alec Radford, Ilya Sutskever, and Dario Amodei. 2020. [Language models are few-shot learners](#).
- Matthieu Courbariaux, Itay Hubara, Daniel Soudry, Ran El-Yaniv, and Yoshua Bengio. 2016. [Binarized neural networks: Training deep neural networks with weights and activations constrained to +1 or -1](#).
- Emily Dinan, Varvara Logacheva, Valentin Lialykh, Alexander Miller, Kurt Shuster, Jack Urbanek, Douwe Kiela, Arthur Szlam, Iulian Serban, Ryan Lowe, Shrimai Prabhumoye, Alan W Black, Alexander Rudnicky, Jason Williams, Joelle Pineau, Mikhail Burtsev, and Jason Weston. 2019. [The second conversational intelligence challenge \(convai2\)](#).
- Josip Djolonga, Mario Lucic, Marco Cuturi, Olivier Bachem, Olivier Bousquet, and Sylvain Gelly. 2020. [Precision-Recall Curves Using Information Divergence Frontiers](#). In *International Conference on Artificial Intelligence and Statistics*, pages 2550–2559.
- Angela Fan, Mike Lewis, and Yann N. Dauphin. 2018. [Hierarchical Neural Story Generation](#). In *Proc. Association for Computational Linguistics*, pages 889–898.
- Ian J. Goodfellow, Jean Pouget-Abadie, Mehdi Mirza, Bing Xu, David Warde-Farley, Sherjil Ozair, Aaron Courville, and Yoshua Bengio. 2014. [Generative adversarial networks](#). In *Proc. of NeurIPS*.
- Perttu Hämmäläinen and Arno Solin. 2020. [Deep Residual Mixture Models](#). *arXiv preprint arXiv:2006.12063*.
- Martin Heusel, Hubert Ramsauer, Thomas Unterthiner, Bernhard Nessler, and Sepp Hochreiter. 2017. [Gans trained by a two time-scale update rule converge to a local nash equilibrium](#). In *Proc. of NeurIPS*, page 6629–6640, Red Hook, NY, USA. Curran Associates Inc.

- Ari Holtzman, Jan Buys, Maxwell Forbes, and Yejin Choi. 2020. [The Curious Case of Neural Text De-generation](#). In *International Conference on Learning Representations*.
- Daphne Ippolito, Daniel Duckworth, Chris Callison-Burch, and Douglas Eck. 2020. [Automatic detection of generated text is easiest when humans are fooled](#). In *Proceedings of the 58th Annual Meeting of the Association for Computational Linguistics*, pages 1808–1822, Online. Association for Computational Linguistics.
- Jeff Johnson, Matthijs Douze, and Hervé Jégou. 2019. Billion-scale similarity search with GPUs. *IEEE Transactions on Big Data*.
- Tuomas Kynkäänniemi, Tero Karras, Samuli Laine, Jaakko Lehtinen, and Timo Aila. 2019. [Improved precision and recall metric for assessing generative models](#). In *NeurIPS*.
- Chin-Yew Lin. 2004. [ROUGE: A package for automatic evaluation of summaries](#). In *Text Summarization Branches Out*, pages 74–81.
- Pedro Henrique Martins, Zita Marinho, and André F. T. Martins. 2020. Sparse Text Generation. In *Conference on Empirical Methods in Natural Language Processing*, pages 4252–4273.
- Luca Massarelli, Fabio Petroni, Aleksandra Piktus, Myle Ott, Tim Rocktäschel, Vassilis Plachouras, Fabrizio Silvestri, and Sebastian Riedel. 2019. How Decoding Strategies Affect the Verifiability of Generated Text. *arXiv preprint arXiv:1911.03587*.
- Nitika Mathur, Timothy Baldwin, and Trevor Cohn. 2020. [Tangled up in BLEU: Reevaluating the evaluation of automatic machine translation evaluation metrics](#). In *Proceedings of the 58th Annual Meeting of the Association for Computational Linguistics*, pages 4984–4997, Online. Association for Computational Linguistics.
- Kaisa Miettinen. 2012. *Nonlinear Multiobjective Optimization*, volume 12. Springer Science & Business Media.
- Kishore Papineni, Salim Roukos, Todd Ward, and Wei-Jing Zhu. 2002. [Bleu: a method for automatic evaluation of machine translation](#). In *Proceedings of the 40th Annual Meeting of the Association for Computational Linguistics*, pages 311–318, Philadelphia, Pennsylvania, USA. Association for Computational Linguistics.
- Ben Peters, Vlad Niculae, and André F. T. Martins. 2019. [Sparse sequence-to-sequence models](#). In *Proceedings of the 57th Annual Meeting of the Association for Computational Linguistics*, pages 1504–1519, Florence, Italy. Association for Computational Linguistics.
- Alec Radford, Jeffrey Wu, Rewon Child, David Luan, Dario Amodei, and Ilya Sutskever. 2019. [Language models are unsupervised multitask learners](#). *OpenAI blog*, 1(8):9.
- Alexandre Sablayrolles, Matthijs Douze, Cordelia Schmid, and Hervé Jégou. 2019. Spreading vectors for similarity search. In *International Conference on Learning Representations*.
- Mehdi S. M. Sajjadi, Olivier Bachem, Mario Lucic, Olivier Bousquet, and Sylvain Gelly. 2018. [Assessing generative models via precision and recall](#). In *NeurIPS*.
- Tim Salimans, Ian Goodfellow, Wojciech Zaremba, Vicki Cheung, Alec Radford, and Xi Chen. 2016. [Improved techniques for training GANs](#).
- Sean Welleck, Ilia Kulikov, Jaedeok Kim, Richard Yuanzhe Pang, and Kyunghyun Cho. 2020a. Consistency of a recurrent language model with respect to incomplete decoding. In *Conference on Empirical Methods in Natural Language Processing*, pages 5553–5568.
- Sean Welleck, Ilia Kulikov, Stephen Roller, Emily Dinan, Kyunghyun Cho, and Jason Weston. 2020b. Neural text generation with unlikelihood training. In *International Conference on Learning Representations, ICLR 2020*.
- Thomas Wolf, Lysandre Debut, Victor Sanh, Julien Chaumond, Clement Delangue, Anthony Moi, Pierric Cistac, Tim Rault, Rémi Louf, Morgan Funtowicz, Joe Davison, Sam Shleifer, Patrick von Platen, Clara Ma, Yacine Jernite, Julien Plu, Canwen Xu, Teven Le Scao, Sylvain Gugger, Mariama Drame, Quentin Lhoest, and Alexander M. Rush. 2020. Transformers: State-of-the-art natural language processing. In *Empirical Methods in Natural Language Processing*, pages 38–45.
- Tianyi Zhang, Varsha Kishore, Felix Wu, Kilian Q Weinberger, and Yoav Artzi. 2020. [BERTScore: Evaluating text generation with BERT](#). In *Proc. of ICLR*.
- Yaoming Zhu, Sidi Lu, Lei Zheng, Jiaxian Guo, Weinan Zhang, Jun Wang, and Yong Yu. 2018. [Texygen: A benchmarking platform for text generation models](#).

## A Background: Decoding for Natural Language Generation

We start by revisiting some preliminaries for text generation (§A.1), and common decoding strategies (§A.2).

### A.1 Preliminaries

Consider a fixed and finite set  $Y$  of tokens. Let  $\mathcal{Y}$  denote the set of all sequences from  $Y$  of maximal length  $N$ :  $\mathcal{Y} = \cup_{n=1, \dots, N} Y^n$ . We denote such a sequence as  $y = (y_1, \dots, y_n)$ .

Let  $Q(y_i|y_{<i}, x)$  denote a model over a token  $y_i$  given previous tokens  $y_{<i}$  and a context  $x \in \mathcal{X}$ . In the generation task under consideration here, the context could be provided by the generation prompt. The induced distribution over sequences is then

$$Q(y_1, \dots, y_n|x) \propto \prod_{i=1}^n Q(y_i|y_{<i}, x). \quad (1)$$

Let  $\mathcal{P}(Y)$  denote the set of probability distributions over  $Y$ .

### A.2 Decoding: Summary

Neural text generation methods employ two types of decoding based on either (a) sampling, or, (b) maximization. Each decoding method constructs a distribution  $P \in \mathcal{P}(\mathcal{Y})$ . A sampling-based decoder samples from this distribution to generate text, while a maximization-based decoder typically finds the mode of  $P$  (or approximate it). The methods are summarized in Table 7.

**Original Distribution** A sampling-based decoder samples from the learned distribution  $Q$  to generate text, while a maximization-based decoder typically finds the mode of  $Q$  (or approximates it). Greedy decoding employs maximization, i.e. it picks the candidate with the highest probability at a given timestep. Beam search generalizes over greedy by maintaining a beam of size  $b$  over a few time steps, selecting the best candidate from the beam at a given time. Both these approaches employ local approximations, since it is intractable to perform exact maximization. Sampling approaches are, on the other hand, non-deterministic. Pure sampling simply samples a token from  $Q$  at every timestep. While pure sampling might produce diverse text, it can also generate either very generic text, or even incorrect tokens (according to humans) due to the miscalibration of  $Q$  (Braverman et al., 2019) on infrequently seen data.<sup>6</sup>

**Modified Distribution** More recently, decoding strategies that modify  $Q$  to remove low probability events before sampling, have been proposed. Sampling with temperature (Ackley et al., 1985) transforms the distribution to favor more high probability events. Top- $k$  sampling (Fan et al., 2018) involves sampling from a subset of candidates which have the  $k$  highest probabilities; greedy decoding is a special case of this where  $k = 1$ . Nucleus or top- $p$  sampling (Holtzman et al., 2020) involves sampling from the nucleus of the distribution, i.e. only considering the smallest number of candidates whose cumulative probabilities sum up to  $p$  at every timestep. In contrast to the above methods which modify the trained distribution for generation, Martins et al. (2020) propose entmax sampling, which samples from a sparse distribution, trained natively to discard tokens undesirable for diverse, non-repetitive generations.

### A.3 Sampling-Based Decoders

Sampling-based decoding algorithms depend on a recalibration function  $\sigma : \mathcal{P}(Y) \rightarrow \mathcal{P}(Y)$ . They generate a sequence by sampling from a distribution  $\sigma \circ p \in \mathcal{P}(\mathcal{Y})$  over sequences defined as

$$(\sigma \circ p)((y_1, \dots, y_n)|x) = \prod_{i=1}^n \sigma(Q(y_i|y_{<i}, x)).$$

Algorithmically, this is simply obtained by forward sampling as

$$y_i \sim \sigma(Q(\cdot|y_{<i}, x)),$$

---

<sup>6</sup>Note that here we refer to tokens “rare” under the conditional distribution, given the context, as opposed to the marginal distribution.

Decoding Algorithm	Type	Parameters	$[\sigma(\pi)]_j$ definition (upto normalization)
Pure Sampling	Sampling	-	$\pi_j$
Top- $K$ (Fan et al., 2018)	Sampling	Integer $K$	$\pi_j \mathbb{I}(j \in \arg \text{top } k_K(\pi))$
Nucleus (Holtzman et al., 2020)	Sampling	$\rho \in (0, 1)$	$\pi_j \mathbb{I}(j \in \arg \text{top prob}_\rho(\pi))$
Consistent Top- $K$ (Welleck et al., 2020a)	Sampling	Integer $K$	$\pi_j \mathbb{I}(j \in \arg \text{top } k_K(\pi) \cup \{j_{\text{eos}}\})$
Consistent Nucleus (Welleck et al., 2020a)	Sampling	$\rho \in (0, 1)$	$\pi_j \mathbb{I}(j \in \arg \text{top prob}_\rho(\pi) \cup \{j_{\text{eos}}\})$
Sparsemax (Martins et al., 2020)	Sampling	-	$\pi_j$ , where $p(\cdot y_{<t}, x)$ is parameterized differently
Greedy	Deterministic	-	$\mathbb{I}(j \in \arg \max_i \pi_i)$
Beam Search	Deterministic	-	See Text
Delayed Beam Search (Massarelli et al., 2019)	Sampling	Prefix length $L$	$\pi_j$ , where Sampling for $L$ steps followed by beam search

Table 7: A survey of different decoding algorithms used in sampling.

where we denote  $y_{<1} = \emptyset$ . Below, we let  $\pi$  denote the next token distribution. We consider common decoding strategies which fall into this framework.

- Pure sampling, where  $\sigma(\pi) = \pi$ .
- Top- $K$  (Fan et al., 2018), which uses an integer  $K$  as a parameter to define

$$[\sigma_K(\pi)]_j \propto \begin{cases} \pi_j, & \text{if } j \in \arg \text{top } k_K(\pi) \\ 0 & \text{else} \end{cases}.$$

Here,  $\arg \text{top } k_K(\pi)$  denotes the set of  $K$  largest indices of  $\pi$ ,

- Nucleus (top- $\rho$ ) sampling (Holtzman et al., 2020), which uses a parameter  $\rho \in (0, 1]$  to define

$$[\sigma_{\text{nuc}, \rho}(\pi)]_j \propto \begin{cases} \pi_j, & \text{if } j \in \arg \text{top prob}_\rho(\pi) \\ 0 & \text{else} \end{cases}.$$

Here,  $\arg \text{top prob}_\rho(\pi)$  denotes the smallest set of indices of  $\pi$  whose sum is at least  $\rho$ . Formally,  $\arg \text{top prob}_\rho(\pi)$  is the smallest set  $J \subset Y$  such that

$$\sum_{j \in J} \pi_j \geq \rho.$$

- Greedy decoding is a special case of top- $K$  decoding with  $K = 1$ .
- Consistent alternatives to top- $K$  and nucleus sampling (Welleck et al., 2020a) fall into this framework with  $[\sigma_{\text{con}, K}(\pi)]_j$  and  $[\sigma_{\text{con}, \text{nuc}, \rho}(\pi)]_j$  including  $j_{\text{eos}}$ , the special end of sentence token, in the top- $K$  or top- $\rho$  set.
- The entmax sampler (Martins et al., 2020) is pure sampling, which corresponds to  $\sigma(\pi) = \pi$  in this framework. However, we note that the way the entmax sampler is not parameterized using the softmax.

#### A.4 Deterministic Decoders

Deterministic decoders deterministically search through the output space  $\mathcal{Y}$  to produce an output  $y \in \mathcal{Y}$ . In general, deterministic decoders aim towards maximization, i.e., to compute the mode  $\arg \max_{y \in \mathcal{Y}} Q(y|x)$ , of the distribution  $Q(\cdot|x)$ . However, one must resort to approximations since the argmax cannot be computed exactly in a tractable manner, in general. Instances of maximization-based deterministic decoding algorithms include:

- Greedy decoding, which constructs  $\bar{y} \in \mathcal{Y}$  incrementally as

$$\bar{y}_t = \arg \max_{j \in Y} Q(j|\bar{y}_{<t}, x),$$

where we denote  $\bar{y}_{<1} = \emptyset$ .

- Beam Search maintains, in iteration  $t$ , a set  $B_t$  (called the *beam*) of the  $K$ -highest probability prefixes of length  $t$ . Formally, starting with  $B_0 = \emptyset$ , the beam  $B_t$  in iteration  $t$  is generated from the previous beam  $B_{t-1}$  as

$$B_t = \arg \text{top } k_K \{p(y|x) : y \in B_{t-1} \times Y\}.$$

Finally, beam search returns the highest scoring sequences  $\arg \max_{y \in B_N} Q(y|x)$  from the final beam  $B_N$ . Other variants of beam search aim to promote diversity, penalize repetitiveness and encourage longer sentences.

## B Pareto Optimality of Divergence Curves

Here, we show the property of Pareto optimality of  $\mathcal{C}(P, Q)$ . The main property we will show in this section is the following. The proof is at the end of the section.

**Proposition 2.** *Consider two distributions  $P, Q$  with finite support and a scaling constant  $c > 0$ . Let  $R_\lambda$  be such that  $(e^{-c \text{KL}(Q|R_\lambda)}, e^{-c \text{KL}(P|R_\lambda)}) \in \mathcal{C}(P, Q)$ . Then,  $R_\lambda$  is Pareto-optimal for the pair of objectives  $(\text{KL}(Q|\cdot), \text{KL}(P|\cdot))$ . In other words, there does not exist distribution  $R$  such that  $\text{KL}(Q|R) < \text{KL}(Q|R_\lambda)$  and  $\text{KL}(P|R) < \text{KL}(P|R_\lambda)$  simultaneously.*

*Proof.* Let  $\mathcal{F}(P, Q)$  be the Pareto frontier of  $(\text{KL}(Q|\cdot), \text{KL}(P|\cdot))$ . From (Miettinen, 2012, Thm. 3.4.5, 3.5.4), it follows that

$$\mathcal{F}(P, Q) = \left\{ (\text{KL}(P|R_\lambda^*), \text{KL}(Q|R_\lambda^*)) : \lambda \in [0, 1] \right\}$$

where

$$R_\lambda^* \in \arg \min_R \{ \lambda \text{KL}(Q|R) + (1 - \lambda) \text{KL}(P|R) \}.$$

We invoke the next lemma to show that  $R_\lambda^* = \lambda P + (1 - \lambda)Q$  to complete the proof.  $\square$

**Lemma 3.** *Let  $P, Q, S$  be discrete distributions with finite support. For any  $\lambda \in [0, 1]$  and  $\bar{\lambda} = 1 - \lambda$ , letting  $R_\lambda = \lambda P + \bar{\lambda}Q$ , we have the identity*

$$\lambda \text{KL}(P|S) + \bar{\lambda} \text{KL}(Q|S) = \lambda \text{KL}(P|R_\lambda) + \bar{\lambda} \text{KL}(Q|R_\lambda) + \text{KL}(R_\lambda|S).$$

Consequently, we have that

$$R_\lambda \in \arg \min_S \{ \lambda \text{KL}(P|S) + \bar{\lambda} \text{KL}(Q|S) \}.$$

*Proof.* By adding and subtracting  $\sum_i R_{\lambda,i} \log(R_{\lambda,i})$ , we get,

$$\begin{aligned} \lambda \text{KL}(P|S) + \bar{\lambda} \text{KL}(Q|S) &= \sum_i \lambda P_i \log P_i + \bar{\lambda} Q_i \log Q_i - R_{\lambda,i} \log S_i \\ &= \sum_i \lambda P_i \log \frac{P_i}{R_{\lambda,i}} + \bar{\lambda} Q_i \log \frac{Q_i}{R_{\lambda,i}} + R_{\lambda,i} \log \frac{R_{\lambda,i}}{S_i} \\ &= \lambda \text{KL}(P|R_\lambda) + \bar{\lambda} \text{KL}(Q|R_\lambda) + \text{KL}(R_\lambda|S). \end{aligned}$$

The first two terms are independent of  $S$  and the last term is minimized at  $S = R_\lambda$ .  $\square$

**Connection to (Djolonga et al., 2020)** The Pareto frontier  $\mathcal{F}(P, Q)$  of  $(\text{KL}(Q|\cdot), \text{KL}(P|\cdot))$  (defined in the proof of Proposition 2) coincides exactly with the notion of a *inclusive divergence frontier*, as defined by (Djolonga et al., 2020). It follows that the inclusive divergence frontier is related to the divergence curve we have defined as,

$$\mathcal{F}(P, Q) = \left\{ (c^{-1} \log t_1^{-1}, c^{-1} \log t_2^{-1}) : (t_1, t_2) \in \mathcal{C}(P, Q) \right\}.$$

## C Additional Details of Experiments

### C.1 Training Hyperparameters

**Web Text** We use a pre-trained GPT-2 model to generate web text. In addition, we also consider entmax sampling (Martins et al., 2020), which is finetuned using the entmax loss; we use the authors’ code<sup>7</sup>. We finetune GPT-2 large on the training set of web text with the entmax loss with an effective batch size of 32 for one epoch. The learning rate and optimizer was default used by Martins et al. (2020), i.e., the Adam optimizer with a learning rate of  $6.25 \times 10^{-5}$ , which was linearly decayed to zero over the course of training. We used a block size of 512.

**Story Continuation** We finetune GPT-2 medium on the training set of the WritingPrompts dataset using the cross entropy loss for one epoch over the training set with an effective batch size of 32 and a block size of 512. We use the default optimizer and learning rate schedules of the HuggingFace Transformers library, i.e., the Adam optimizer with a learning rate of  $5 \times 10^{-5}$ . In addition, we also finetune GPT-2 medium with the entmax loss in order to use the entmax sampler (Martins et al., 2020). The finetuning settings are identical to those described in the previous paragraph.

### C.2 MAUVE Hyperparameters

**MAUVE- $k$ -means** We first run PCA on the data matrix obtained from concatenating the hidden state representations of the human text and model text. We keep 90% of the explained variance and normalize each datapoint to have unit  $\ell_2$  norm. We then run  $k$ -means with FAISS for a maximum of 500 iterations for 5 redos. We quantize represent the human text distribution and the model text distribution by a histogram obtained from cluster memberships.

**MAUVE-DRMM** We use the code released by the authors<sup>8</sup>. We take 10 components per layer and 3 layers for a total of 100 layers. We train the DRMM for 20 epochs using a batch size of 64 and an initial learning  $\gamma_0$  of 0.005. The learning rate  $\gamma_t$  used is

$$\gamma_t = \gamma_0 \min\{1, (2 - 2t/T)^2\},$$

where  $T$  is the total number of updates. That is, it is set constant for the first half of the updates and then annealed quadratically. For more details, see (Hämäläinen and Solin, 2020, Appendix C).

**MAUVE-Lattice** We use the code provided by the authors<sup>9</sup>. We train a 4-dimensional feature representation of the hidden states for 200 epochs using the triplet loss of (Sablayrolles et al., 2019), so that the learnt feature representations are nearly uniformly distributed. We use a 2-layer multilayer perceptron with batch normalization to learn a feature representation. We train this MLP for 200 epochs with batch size of 64 and an initial learning rate of 0.1. The learning rate is cut to 0.05 after half the training and 0.01 after 75% of the training.

The learnt feature representations are then quantized using the lattice spherical quantizer into 744 bins. This work as follows: let  $S_r$  denote the integral points of the unit sphere of radius  $r = \sqrt{50}$  in  $\mathbb{R}^4$ . A hidden state vector  $x$  is run through the trained MLP  $f$  to get its feature representation  $f(x)$ . It is quantized to the bucket  $u$  given by

$$\mathcal{I}(x) = \arg \min_{u \in S_r} \|r \times f(x) - u\|_2^2.$$

---

<sup>7</sup>[https://github.com/deep-spin/sparse\\_text\\_generation](https://github.com/deep-spin/sparse_text_generation)

<sup>8</sup><https://github.com/PerttuHamalainen/DRMM>

<sup>9</sup><https://github.com/facebookresearch/spreadingvectors>